Biogeosciences Discuss., 9, 10241–10283, 2012
www.biogeosciences-discuss.net/9/10241/2012/
doi:10.5194/bgd-9-10241-2012

Biogeosciences Discussions

Carbon fluxes forced by anticyclonic mesoscale eddies generated by islands at the subtropical NE Atlantic Ocean

S. Lasternas[1], M. Piedeleu[2], P. Sangrà[2], C. M. Duarte[1,3], and S. Agustí[1,4]

[1]Global Change Research Department, IMEDEA (CSIC-UIB), Miquel Marqués 21, 07190 Esporles, Spain
[2]Instituto Universitario de Oceanografía y Cambio Global (IOCAG-ULPGC), Universidad de Las Palmas de Gran Canaria, Las Palmas de Gran Canaria, Spain
[3]The UWA Oceans Institute, The University of Western Australia, 35 Stirling Highway, 6009 Crawley, Australia
[4]The UWA Oceans Institute and School of Plant Biology, The University of Western Australia, 35 Stirling Highway, 6009 Crawley, Australia

Received: 10 July 2012 – Accepted: 24 July 2012 – Published: 3 August 2012

Correspondence to: S. Lasternas (sebastien@imedea.uib-csic.es)

Published by Copernicus Publications on behalf of the European Geosciences Union.

Abstract

The carbon fluxes mediated by planktonic communities in two cyclonic eddies (CEs) and two anticyclonic eddies (AEs) at the Canary Eddy Corridor were studied and compared with the dynamics in two far-field (FF) stations located outside the eddies. We observed favorable conditions and signs for upwelling at the center of CEs and for downwelling and mixing at the centers of AEs. CEs were characterized by higher nutrients concentration and highest chlorophyll *a* concentration, associated with highest microphytoplankton and diatoms abundance. AEs displayed similar chlorophyll *a* values and nutrients concentration (except highest ammonium concentration) to those of the FF stations and were characterized by increasing abundance of picophytoplankton and heterotrophic bacteria. While primary production was similar between the systems, the production of dissolved organic carbon (P_{DOC}) was significantly higher at AEs. Phytoplankton cell mortality was lowest in CEs and we found higher cell mortality in AE than FF, despite similar chl *a* concentration. Environmental changes at the AEs presented significant prejudicial effects on the phytoplankton health as indicated by higher phytoplankton mortality (e.g. 60 % of dead diatoms cells) and higher cell lysis rates observed at AEs than at two other systems. The adverse conditions associated to the early-stage anticyclonic systems, mainly triggered by active downwelling, resulted in higher consequent P_{DOC} production, corresponding to forcing of the carbon flux to the dissolved pool and a weakness of the carbon pump.

1 Introduction

Mesoscale eddies dynamics exert profound influences on the vertical fluxes of organic matter, nutrients and carbon (Owen, 1981; Arístegui et al., 2003; Martin and Richards, 2001; Mathis et al., 2007; Alonso-González et al., 2010; Benitez-Nelson and McGillicuddy, 2008) and may modulate the Oceanic Vertical Pump (VOP) (Oschlies and Garçon, 1998). Previous studies have indicated the importance of mesoscale

BGD
9, 10241–10283, 2012

eddies in ocean biogeochemistry by modulating the efficiency of the biological pump. Indeed, cyclonic eddies (CEs) tend to promote the biological pump by increasing nutrient supply, thereby enhancing the primary production (Smith et al., 1996; Garçon et al., 2001; McGillicuddy et al., 2007) and by favouring larger phytoplankton cells (Rodriguez et al., 2001; Vaillancourt et al., 2003). Anticyclonic systems are mostly oligotrophic structures characterized by nutrient-poor surface waters (Falkowski et al., 1991; McGillicuddy et al., 1998), constraining primary production and frequently associated with relatively intense bacterial abundance and production (Bidigare et al., 2003; Ewart et al., 2008; Baltar et al., 2010).

Surface anticyclonic eddies may also enhance phytoplankton abundances and biomass (McGillicuddy et al., 2007; Sangrà et al., 2009) through ageostrophic secondary circulation (ASC) forced by non-linear advection effects on the surface wind stress (Hart, 1996). One approach to examine these effects integrates this eddy-wind interaction along the whole eddy (McGillicuddy et al., 2007; Martin and Richards, 2001) while other considers the details at the periphery (Mahadevan et al., 2007). The first approach results in an upwelling at the eddy center and the second in an upwelling/downwelling vertical ASC cell at the periphery as reported in narrow frontal regions (Pallàs-Sanz et al., 2010). Both approaches require and uniform wind blowing over the eddy and are linked to a non-linear Ekman surface-layer pumping as consequence of the flow-wind interaction (Hart, 1996). For eddies located near the lee of Tall Deep Islands this is not the case as two counter rotating cells wind wake develops creating strong wind shears that forces linear Ekman pumping velocities (Jiménez et al., 2008; Jia et al., 2011). The anticyclonic/cyclonic cell forces upwelling/downwelling that may promote AEs/CEs generation driving the ASC at their initial stages. During their spin up time an upwelling/downwelling may originate in CEs/AEs eddies being the opposite during the spin-down time (McNeil et al., 1999; McGillicuddy et al., 1998). Regardless of whether these mechanisms are primarily controlling the VOP dynamics, their occurrence at AEs suggests probably higher dynamics than that reflected in the production of biomass.

BGD
9, 10241–10283, 2012

The Canary Archipelago is a continuous source of mesoscale eddies generated by the Canary Current and Trade Wind perturbation by the islands topography (Jiménez et al., 2008; Piedeleu et al., 2009) and the main pathway of long lived eddies in the North East Subtropical Atlantic originating the Canary Eddy Corridor (Sangrà et al., 2009). La Palma, El Hierro, Tenerife and Gran Canaria Islands, where surveyed eddies have been located, may be viewed as Tall Deep Islands due to their step and higher topography. It has been documented the presence of a strong surface wind shear/curl cells at these islands lees during summer (Basterretxea et al., 2002; Jiménez et al., 2008; Mason et al., 2001). On the basis of a submesoscale resolution quasi-synoptic temperature section crossing the Gran Canaria wake, Basterretxea et al. (2002) observed evidences of downward/upward lineal Ekman surface-layer pumping coinciding with strong anticyclonic/cyclonic wind shear regions. Additional studies have been initiated at this zone to better understand the implication of counter-paired cyclonic and anticyclonic eddies for biological processes and to address their influence in carbon fluxes. Cyclonic eddies promoted nutrient pumping and vertical uplifting of the deep chlorophyll maximum, increasing plankton production, while anticyclonic eddies tended to accelerate downstream transport below the photic zone (Arístegui et al., 1997; Arístegui and Montero, 2005; González-Dávila et al., 2006). Since anticyclonic structures can be long lived coherent structures lasting several months (Sangrà et al., 2005, 2009), the magnitude and the efficiency of the biological pump can be affected for extended periods and may consequently have significant implications in carbon fluxes.

In the present study, we aim to explore whether anticyclonic eddies may affect the physiological status of phytoplankton and heterotrophic bacteria cells by stressing populations as a consequence of the downstream processes and associated nutrient concentrations decline. We do so by characterizing the hydrological conditions and physical features of the eddy systems along with the nutrient availability and biological processes at the euphotic zone within cyclonic and anticyclonic systems of the Canary eddy fields and by comparing to similar processes in waters outside the eddies system. Specifically, we quantify the abundance and physiological status of heterotrophic

BGD
9, 10241–10283, 2012

bacteria and phytoplankton and its community structure, as well as the production of dissolved organic carbon, linking these two components of the planktonic food web.

The status of phytoplankton cells is emerging as a key driver determining the flow of carbon from primary producers to phytoplankton, indicated by phytoplankton mortality and cell lysis during stress (e.g. Agustí et al., 2001). Both mechanisms are perceived to be important loss processes (Proctor and Fuhrman, 1991; Brussaard et al., 1995; Agustí and Duarte, 2000) and increase the proportion of primary production that flows to the dissolved pool as dissolved organic carbon production (P_{DOC}). Phytoplankton health status is likely dependent on the presence of stressors, such as reduced nutrient availability (Myklestad, 1977), or incident UVB and PAR radiation (Berges and Falkowski, 1998; Llabrés and Agustí, 2006). Hence, changes in hydrological properties occurring at anticyclonic systems, affecting nutrient availability of the exposure of phytoplankton cells to intense UVB and PAR radiation, may stress phytoplankton cells resulting in subsequent losses through cell mortality and lysis.

The examination of the physiological status of phytoplankton and bacteria cells in eddy systems may, therefore, provide insights into the consequence of eddy dynamics for carbon fluxes in the ocean. We, therefore, examined anticyclonic and cyclonic eddies in the Canary eddy field to test for differences in the flow of carbon and physiological status of phytoplankton and heterotrophic bacteria. In particular, we examined particulate and dissolved primary production, phytoplankton lysis rates, the percentage of living and dead phytoplankton and heterotrophic bacteria cells. We examine here the relationship between phytoplankton cell mortality and lysis rates and the production of dissolved organic carbon by phytoplankton (P_{DOC}) and their relationship with the status of bacteria cells. We examined these properties in two anticyclonic and two cyclonic eddies in the Canary eddy field as well as two far-field locations to examine these properties in the absence of eddy forcing.

BGD
9, 10241–10283, 2012

2 Material and method

2.1 Cruise track and eddies description

Sampling was conducted at stations located at the subtropical northeast Atlantic, in the Canary Islands region (Fig. 1), on board the R/V *Hespérides* during the RODA-1 (Remolinos Oceánicos y Deposición Atmosférica) cruise from 11 August to 5 September 2006. The biological and chemical characteristics of eddies were studied in two cyclonic eddies (CE1, CE2), two anticyclonic eddies (AE1, AE2), and two stations away from the perturbed region by the Island, named as undisturbed far-field stations (FF1, FF2; Fig. 1). To identify the eddy fields and investigate the initial hydrographic structure of cyclonic and anticyclonic eddies shed by the Canary Islands, their lee waters were first surveyed using real-time sea surface temperature (SST). These images allowed to detect the surface signature of four eddies; two cyclonic eddies, one in the lee of Gran Canaria (CE1), another west of La Palma (CE2) and two anticyclonic eddies, located southeast of El Hierro (AE1) and southwest of Gran Canaria (AE2) (Fig. 1). During each survey we sampled sections of 9 to 13 expendable bathythermograph (XBT) or CTD stations across the estimated eddy centers. The XBT probes provide the temperature of the water column down to a depth of 700 m while CTD probes reached 1000 m depth (Figs. 2a, d, 3a, d). Temperature anomalies were calculated using as reference the most distant section stations from the eddy centers, where minimums in the isotherm perturbation were encountered (Figs. 2b, e, 3b, e). These parameters were used to estimate the eddy maximum depths and the diameter of the mesoscale structures (Table 1). The same method as temperature anomalies have been used to calculate depth anomalies, the latter provide valuable information on the intensity of eddies. Mixed layer depths were calculate using Kara et al. (2000) method and checked visually. Wind curl fields were derived from Cross-Calibrated Multi-Plataform gridded surface wind vectors field (CCMP-Winds) provided by PODAAC/JPL-NASA (http://podaac.jpl.nasa.gov/DATA_CATALOG/ccmpinfo.html) and a level 3.5a product, that are 0.25° gridded data 5 days averaged and includes QuickScat data, was used.

BGD
9, 10241–10283, 2012

Instantaneous wind vectors were also derived along the eddies transects from the on-board meteorological station.

2.2 Biogeochemical sampling

At the 6 stations (CE1-CE2, AE1-AE2 and FF1-FF2), vertical profiles of temperature, salinity, and fluorescence down to 200 m depth were performed using a Seabird 911 Plus conductivity-temperature-depth (CTD) system. The fluorescent profiles were used to estimate the deep chlorophyll maximum (DCM) depths. Seawater samples were collected in 12-l Niskin bottles mounted on a General Oceanics rosette sampler, at an average of 5 depths from the surface to 200 m. Samples for nutrient analysis (phosphate, nitrate + nitrite, ammonium and silicate) were collected down to 200 m. Samples for the determination of the dissolved inorganic phosphate concentrations and the nitrate + nitrite concentrations were kept frozen until analyzed in a Bran + Luebbe AA3 auto-analyzer following standard spectrophotometric methods (Hansen and Koroleff, 1999) and ammonium concentrations were measured spectrofluorometrically within 1 h of collection following Kérouel and Aminot (1997).

Samples of 200 ml of water were filtered through Whatmann GF/F filters to estimate total chlorophyll *a* concentration (Chl *a*) and extracted for 24 h in 90 % acetone fluorometric determination (Turner Designs fluorometer) following Parsons et al. (1984).

Samples for the quantification of nano and microphytoplankton abundance were sampled at surface (5 m) and the deep chlorophyll maximum (DCM). Samples of 2–3 l were concentrated onto 50–70 ml samples by using a Millipore cell concentrator chamber, which allows concentration of cells with no significant effect on cellular status (e.g. viability, movement for flagellated cells, integrity of frustules) (Agustí and Sánchez, 2002; Alonso-Laita and Agustí, 2006; Lasternas et al., 2010). 10 ml aliquots (duplicates) of the resulting concentrate were filtered onto 2 µm pore-size black polycarbonate filters, fixed with gluteraldehyde (1 % final concentration) and stored frozen at −80 °C until counting. Phytoplankton cells were counted using an epifluorescence microscope (Zeissé Axioplan Imaging), and were classified into 3 majors groups,

BGD
9, 10241–10283, 2012

nanoflagellates, dinoflagellates and diatoms, which were separated into pennate and centric.

Autotrophic picoplankton abundance was assessed using Flow Cytometry. At each station, duplicated 2 ml fresh samples from 5 depths were counted on board (duplicated counts) using a FACSCalibur Flow Cytometer (Beckton Dickinson). An aliquot of a calibrated solution of 1 µm diameter fluorescent beads (Polysciences Inc.) was added to the samples as an internal standard for the quantification of cell concentration. The red (FL3, bandpass filter 670 nm), green (FL1 bandpass filter 530 nm) and orange (FL2, bandpass filter 585 nm) fluorescence, and forward and side scattering signals of the cells and beads were used to detect picoplanktonic populations of *Synechococcus*, *Prochlorococcus* and eukaryotes (Marie et al., 2005).

The proportion of dead cells in the autotrophic communities examined was quantified by applying a cell membrane permeability test, the cell digestion assay (CDA, Agustí and Sánchez, 2002). The CDA involves the exposure of phytoplankton cells to an enzymatic cocktail (DNAse and Trypsin) that enters the cytoplasm and digests cells with compromised membranes, the dead or dying cells, which are removed from the sample. The cells remaining in the samples after the CDA are the living cells, those with intact membranes, which were then counted by flow cytometry or epifluorescence microscope, as described above (cf. Agustí and Sánchez, 2002). The CDA was applied to the concentrates of nano and microphytoplankton cells prepared to quantify total cell abundance. The cell digestion assay was applied to duplicated 10 ml aliquots of cell concentrate by adding 2 ml of DNAse I solution (400 µg ml^{-1} in HBSS (Hanks' Balanced Salts)), followed by 15 min incubation at 35 °C in a Digital Dry Bath. After this time, 2 ml of Trypsine solution (1 % in HBSS) were added, followed by 30 min incubation at 35 °C. At the end of the incubation, samples were placed in ice in order to stop the enzymatic cell digestion process and were then filtered onto polycarbonate 2 µm pore diameter black filters, washed several times with filtered seawater, fixed with gluteraldehyde (1 % final concentration) and stored frozen at −80 °C until counting by epifluorescence microscopy.

BGD
9, 10241–10283, 2012

Fresh samples to quantify the proportion of living picophytoplankton cells were sampled from the 5 same depths selected to estimate total picoplankton abundance at each station. Duplicated 1 ml samples were run with the CDA, by adding first, 200 µl of DNAse I solution and, after 15 min incubation at 35 °C, 200 µl of Trypsin solution. Treated sampled were incubated for 30 min more at 35 °C and were finally placed in ice in order to cease enzymatic activity. Samples were then counted by flow cytometry as described above for total picophytoplankton abundance estimates. The percentage of dead cells was calculated as the ratio between the concentration of dead cells (total concentration minus concentrations after applying the CDA, living cells) and total population abundance, which includes both living and death cells (Agustí and Sánchez, 2002).

Primary production was assessed by the ^{14}C technique (Steeman-Nielsen, 1952). Seawater initially sampled at 5 depths including the surface (5 m), two intermediate depths, the DCM and an ultimate depth below the DCM, was delivered into transparent (light) and black masking tape-covered polycarbonate bottles (150 ml), and inoculated with 80 µCi activity of a $NaH^{14}CO3$ working solution. Depending on sea conditions the incubations were deployed in a mooring buoy system and incubated in situ for 3 h. For some of the stations, however, the deployment of the buoy was not possible and incubations were performed on deck, using incubators at controlled temperature and adjusting the incident natural irradiance to that received in situ using neutral density screens. The incubations run for 3 h and measurements were limited to 2 depths (Surface and DCM). For each sample, two aliquots of 5 ml (replicates) were introduced in scintillation vials (20 ml) for the determination of total labelled organic carbon production (TPP); the sum of ^{14}C incorporated into POC (particulate organic carbon) and released as DOC (dissolved organic carbon). The remaining volume was filtered through 0.22 µm mesh membrane filters (cellulose membrane filters) of 25 mm ∅ to determine particulate primary production (PPP > 0.22 µm). To remove inorganic ^{14}C, the liquid samples were acidified with 100 µl of 10 % HCl and shacked for 12 h, while the filters were fumed with concentrated HCl (37 %) for 12 h. Then, 10 ml and 5 ml of scintillation cocktail (Packard

BGD
9, 10241–10283, 2012

Ultima Gold XR) were respectively added to TPP and PPP vials and the disintegrations per minute were counted after 24 h with a scintillation counter (EG&G/Wallac). The dissolved organic carbon production by phytoplankton (P_{DOC}) was calculated as the difference between total and particulate primary production and the percentage of the production released extracellular by phytoplankton (PER) was calculated as $(P_{DOC}\,TPP^{-1}) \times 100$.

Phytoplankton cell lysis rates were estimated using the dissolved esterase method as described in Agustí et al. (1998). Dissolved esterase activity (as FDA hydrolysis) was measured in 3 replicates at each depth sampled. In short, 5 ml of water were filtered through 0.2 µm Millipore Millex filters, and 50 µl of EDTA and 50 µl of FDA (Sigma Co.) were added to the samples (to a final concentration of 0.02 and 0.2 mM respectively) and mixed in a vortex mixer. After incubating the samples for an hour at 20 °C, the fluorescence emission was immediately measured in a Shimadzu RF-5000 spectrofluorometer at 451 nm and 510 nm excitation and emission (10 nm bandwidth) wavelengths, respectively. The particulate esterase activity (PEA), needed to estimate the lysis rate, was calculated from the measured chl *a* concentration, using a PEA : chl a ratio of 331 nmol F (µg chl *a*)$^{-1}$ h^{-1} derived from phytoplankton cultures (Agustí and Duarte, 2000). Phytoplankton cell lysis rates (μ_L d^{-1}) were calculated as the decrease in PEA with time due to the production of dissolved esterase activity (EA) during cell lysis. The production of dissolved EA was derived by combining the measured dissolved EA activity with estimates of the rate of loss of the activity of the enzyme calculated experimentally.

At each station, the abundance and the proportion of living heterotrophic bacteria were quantified in samples collected at 5 depths. To do so, we used the Nucleic Acid Double Staining (NADS) flow cytometric protocol (Gregori et al., 2001). This technique involves the use of two nucleic acid fluorescent dyes, SYBR Green I (SG1; Molecular Probes) and Propidium Iodide (PI; Sigma Chemical Co.). Bacterial membranes are permeable to SG1, whatever the cell viability, resulting in green fluorescence when stained. However, living or viable cells, with intact plasmic membranes, are impermeable to PI.

BGD
9, 10241–10283, 2012

Thus only compromised or damaged cells are stained with PI (Barbesti et al., 2000), showing red fluorescence as described in Falcioni et al. (2008). Subsamples were analyzed immediately after collection. Samples (1 ml) were stained with 10 µl of Propidium iodide (PI, 1 mg ml^{-1} stock solution), reaching a final concentration of 10 µg ml^{-1} and incubated for 30 min in dark and room temperature. Then, 10 µl of SYBR Green I (10-fold dilution of 10 000 × commercial solution in dimethyl sulfoxide) were added to subsample and incubated for 10 more minutes. SG1 and PI fluorescence were detected using a FACSCalibur Flow Cytometer (Beckton Dickinsoné) in the green (FL1) and the red (FL3) fluorescence channels, respectively. Bivariate plots of green versus red fluorescence (FL1 vs. FL3) allowed discriminating live (green fluorescent, impermeable to PI) from dead cells (red fluorescent membrane-compromised cells, stained by PI and SG1). Bacteria concentration was calculated using a 1-µm diameter fluorescent bead (Polysciences Inc.) solution as an internal standard. Total heterotrophic bacterial abundance, in cells ml^{-1}, was calculated as the sum of red and green fluorescent cell abundance, while living bacterial cell abundance was determined from the green fluorescent cell counts.

2.3 Data analysis

Spearman's rank coefficients were used to determine correlation between variables that departed from normality (Siegel and Castellan, 1988). Statistical significance of the differences between average values were tested using Student's t-test, with a critical p-value of 0.05.

3 Results

3.1 Hydrophysical eddies structures

Three contrasting zones were characterized during the cruise, the cyclonic and anticyclonic oceanic eddy (CE and AE) fields located at the lee of the Canary Islands and the

BGD
9, 10241–10283, 2012

far-field off the archipelago. Far-field stations were away from the influence of the islands, so probably undisturbed by any eddy (Fig. 1). The depth of the eddies sampled, obtained from the temperature anomalies sections (Figs. 2 and 3), ranged between 300 for AE2 and greater than 500 m for CE1 (Table 1). Previous observations showed that the signature of the eddies can reach at least 700 m hence affecting the whole depth range of the main thermocline occupied by North Atlantic Central Water (Sangrà et al., 2007). Cyclones of La Palma (CE2) and Gran Canaria (CE1) were close to the southwest flank of these islands (Fig. 1) and were samped at their early life stage (spin up stage) having a radius of about 25 km and about 35 km respectively. Anticyclone AE1 probably generated by the island of Tenerife, but located far from this island at the time of sampling and hence relatively older, presented the larger observed radius of about 65 km. Gran Canaria anticyclone, AE2, with a smaller radius of about 50 km, was located close to the island of origin and therefore was probably younger than AE1, being at its early stage of generation (spin up stage). The radius length was calculated as the maximum horizontal extension of the temperature anomaly observed in the vertical sections (Figs. 2 and 3). This should be taken with some caution because as our sampling was based on the SST signal of the eddies, and we cannot be completely sure that the sections crosses exactly the eddy center. The cyclones' signatures were apparent on the temperature sections through the doming of the isotherms introducing negative temperature anomalies in the water column (Fig. 2). The maxima of the temperature anomaly helped us locate the center of the eddies, which was then selected for biogeochemical sampling (stations CE1-CE2 in Fig. 2). Negative temperature anomalies introduced by these cyclones were rather large being approximately 4 °C (Table 1) at 50 m depth. The base of the seasonal thermocline was marked by the 20 °C isotherm (Fig. 2a, d) and its depth just outside the eddies was around 100 m shoaling at the eddy centers until 30 m for CE1 and 50 m for CE2. The maximum isotherm depth anomaly reached 77 m for CE1 and 50 m for CE2 (Table 1).

Anticyclones deepened the isotherms introducing positives anomalies in the temperature field (Fig. 3b, e). As in the case of cyclones the maxima of the temperature

BGD
9, 10241–10283, 2012

anomaly helped us to locate the eddy center. The eddy center of AE1 was well defined by these maxima, which was then selected for biogeochemical sampling for AE1 (Fig. 3b). The vertical section crossing AE2 does not show a well-defined eddy center, however temperature anomalies and depth anomalies sections (Fig. 3e, f) suggested that sampling was not far from the eddy center (Table 1). The 20 °C isotherm deepened 50 m from the eddy periphery to the center in the case of AE1 and 40 m in the case of AE2. In the case of the Canary anticyclones it has been observed that the nutricline deepens accompanying the isopycnal/isotherms.

Mean wind curl obtained from CCMP climatology showed that cyclonic/anticylonic wind curl cells affected the sampled eddies (Fig. 4a, b). According to this, instantaneous wind data recorded along the eddy transects showed also the occurrence of strong wind shears/wind curls (Fig. 4c). CCMP data were five days averaged and must be taken with some caution because their resolution (0.25°) merely resolved the wind curl cells. Therefore a certain divergence may be expected when comparing the location of the maximum instantaneous wind shear/curl from ship observations and from CCMP as in the case for La Palma.

Figure 4 showed a strong wind shear along CE2 (Fig. 4c) related with the relatively strong cyclonic wind curl cell of La Palma (Fig. 4a, b). The maximum cyclonic wind shear/curl was located nears the eddy center (Fig. 4c). A close inspection of Fig. 2d showed a surface outcropping of those isotherms located at the base of the mixed layer, probably corresponding to a water upwelling at the eddy center by the upward Ekman pumping vertical velocity linked with the cyclonic wind curl cell. Despite there were no reliable wind ships observation for eddy CE1, Fig. 4a and b showed a small cyclonic wind curl cell at the eddy location. Therefore as the case of eddy CE2, we encountered favourable conditions for upwelling (upward Ekman velocity), as related to the divergence of the Ekman transport. For the case of eddies AE1 and AE2, averaged CCMP data showed a strong wind curl anticylonic cell at the eddies locations (Fig. 4a, b). Instantaneous ship observations indicated that maximum wind shears/curl were located near the eddies centers (Fig. 4c). The occurrence of a strong anticylonic

BGD
9, 10241–10283, 2012

wind curl/shear indicated that favourable conditions for downwelling (downward Ekman pumping velocity) related with the convergence of the Ekman transport were present.

3.2 Biogeochemical characteristics/properties

Nutrient concentrations were significantly higher at cyclonic than at anticyclonic eddies (Student's t-test, $P < 0.05$; Table 2). Silicate concentration at FF stations was similar to that at CE and higher than that at AE. Concentrations of other nutrient species were significantly lower at FF than at CE (Table 2). AE and FF presented similar DIN and DIP concentrations but for ammonium, with higher concentrations observed at AE than at FF and CE stations. Water temperature at CE was lower on average (Student's t-test, $P < 0.05$; Table 1) than that in the other systems. FF presented a wider gradient of temperature which did not differ significantly in temperature regimes from AE stations (Table 1).

Chlorophyll *a* concentrations presented similar vertical profiles among the two CEs and the two AEs (Fig. 5). Averaged chlorophyll *a* by eddies (CE vs. AE) displayed significantly higher concentration at cyclonic than at anticyclonic systems (Table 2), but were similar in AE and FF. The deep chlorophyll maximum (DCM) was significantly shallower (43.6 ± 0.6 m) at CE (Student's t-test, $P < 0.05$) than at AE (75.5 ± 1.2 m) and FF stations (70 ± 1.3 m). The chlorophyll *a* concentration was positively related to the total phytoplankton biomass, as biovolume ($r_s = 0.36$, $p < 0.05$, df = 12), in the study. At the AE, chlorophyll *a* was positively related to picophytoplankton biovolume ($r_s = 0.63$, $p < 0.05$, df = 12) while at the cyclonic eddies it was associated to microphytoplankton biovolume. The picophytoplankton fraction dominated autotroph communities during the study showing the higher abundances in AE (Fig. 6a). There were no significant differences in the abundance of picophytoplankton groups within the two CEs and the two AEs (Student's t-test, $P < 0.05$). *Prochlorococcus* sp. dominated and was significantly more abundant in AE ($2.2 \pm 0.4 \times 10^5$ cells ml^{-1}). *Synechococcus* sp. presented maximum values at the CE ($6.7 \pm 1.9 \times 10^3$ cells ml^{-1}) although the average abundance did not different significantly between zones. Picoeukaryotes showed

BGD
9, 10241–10283, 2012

contrasting abundance distribution, with higher averaged abundance in CE than at the AE and FF stations.

The microphytoplankton fraction displayed a contrasting pattern with that observed for picophytoplankton. Averaged microphytoplankton abundances were low at FF stations, increasing in AE and been significantly higher at CE stations (Fig. 6b). Nanoflagellates followed a similar trend (Table 3). Diatoms abundances were significantly higher in the CE zone than at the other two systems (Table 3) while dinoflagellates presented similar abundances between the AE and FF stations (Table 3). We observed also contrasting vertical distribution between diatoms and nanoflagellates, with diatoms (mostly centric) prevailing at the surface in AE and at DCM layers at the CE, while nanoflagellates presented an opposite distribution.

Diatoms showed higher averaged % DC at the AE and lowest at the cyclonic eddies (Fig. 7b), with nano and microphytoplankton cells showing a higher proportion of dead cells in AE and low percentages of dead cells at CE (Fig. 7a). The percent of dead picophytoplankton cells ranged broadly, from 16 to 62.3 % of dead cells among communities in the study, and showed also differences between the eddy systems studied, being significantly higher inside the anticyclonic eddies system (Fig. 7c). *Prochlorococcus* sp. presented the lowest percentage of dead cells at the FF stations (42.2 ± 3.4 % DC) while *Synechococcus* sp. and picoeukaryotes displayed the lowest % DC values in the CE system (17.9 ± 6.8 % DC and 25.8 ± 6.1 % DC, respectively).

Particulate primary production (PPP) rates presented low variation (averaging 0.062 ± 0.024 mg C m^{-3} h^{-1}), with no significant differences between zones (Student's t-test, $P < 0.05$). However P_{DOC} production presented significantly higher rates at the AE than at the others areas (Fig. 8a). The percentage of extracellular release by phytoplankton avered 69.5 ± 6.5 % and ranged from 31 to 98 % along the study, with no significant differences between zones. Indeed, phytoplankton cell lysis rates reached also maximum rates at the AE (Fig. 8b) while we observed similar lower values at CE and FF stations. The high mortality of phytoplankton observed at the AE stations (Fig. 7a) was associated with the high production of dissolved organic carbon by phytoplankton

BGD
9, 10241–10283, 2012

(P_{DOC}) in these stations as indicated by the significant positive relationship between lysis rates and P_{DOC} concentration ($R^2 = 0.77$, $p < 0.0005$, df = 12, Fig. 9). The high lysis rates measured at the AE (Fig. 8b) were consistent with the high percentage of dead nano-microphytoplankton cells ($r_s = 0.76$, $p < 0.05$). HB abundance (Fig. 10a) was positively related to P_{DOC} variation ($r_s = 0.65$, $p < 0.05$) and was significantly higher in AE and lower at the FF stations (Fig. 10a). Moreover, HB abundance was significantly associated to NH_4 concentration along the study ($r_s = 0.59$, $p = 0.0069$), and we observed a positive relationship between the percentage of living bacterial cells and NH_4 concentration at AE stations ($R^2 = 0.96$, $p < 0.005$, df = 5). Bacterial viability, presented however similar averages of % LC between anticyclonic and cyclonic eddies and was higher at FF stations (Fig. 10b). Moreover, HB viability was positively related with the percent of dead *Synechococcus* sp. cells ($R^2 = 0.53$, $p < 0.001$, df = 22).

4 Discussion

4.1 Cyclonic eddies

Cyclonic features described during our study supported higher phytoplankton biomass as they enhanced nutrient inputs to the surface, resulting in increased nutrient concentrations, higher chlorophyll *a* concentrations and production rates, as reported for other cyclonic systems (McGillicuddy et al., 1998; Oschlies and Garçon, 1998; Siegel et al., 1999; Tarran et al., 2001). Observed nutrient increase at the center of cyclonic eddies and the corresponding enhancement of phytoplankton abundance detected as in Rodriguez et al. (2003) in the centre of these mesoscale features, may be attributed to both the shoaling of the nutricline and to an upward diapicnal flow (upwelling) The cyclonic wind curl/shear cell that interacts with CEs may cause a divergence of the Ekman transport that leads to an upward Ekman pumping velocity (Jiménez et al., 2008) and hence to favourable upwelling conditions. As already indicated, sign of such upwelling may be inferred from the surface outcropping of the isotherms of the base of mixed

BGD
9, 10241–10283, 2012

layer at the center of CE2 where strong wind shear/curl was observed. Cyclonic eddies were attached at the western flanks of the islands and hence at their early stage of formation. As demonstrated by numerical modelling (Jiménez et al., 2008) upward Ekman velocity is partly responsible for the cyclonic eddies generation and may be very strong at their early stage of generation. Moreover at this spin up stage it may be expected not only a shoaling of the isotherms at the eddy center but also their uplifting that may originate also upwelling. Enhancement of chlorophyll *a* has been recurrently observed at the western flanks of the Canary Island in colour satellite images coinciding with CEs generation (Sangrà et al., 2009). It was mainly observed in those islands with tall and steep topography (La Palmas, Tenerife-La Gomera, El Hierro and Gran Canaria) where strong cyclonic wind curl cells develop at their western flanks.

Besides the enhancement of phytoplankton biomass at CE, the results presented here provide evidence that eddies features also control the community structure and cell status of phytoplankton, as indicated by a significant increase in nano and microphytoplankton abundance at CE waters, especially diatoms, and a decline in the abundance of picophytoplantkonic. Rodriguez et al. (2003) observed that upward velocities favour the growth of large phytoplankton cells, and here, the low microphytoplankton mortality and lower lysis rates observed at cyclonic stations emphasize the favourable growth conditions for large phytoplankton. Therefore the significant increase in diatoms we observed in CE is likely to be related with upward velocity and upwelling dynamics at the center of those structures. Vaillancourt et al. (2003) also observed an increase of microphytoplankton at a cyclonic eddy attached to the Northwest flank of the island of Hawaii, similar to our observations. Jia et al. (2011) recently reported the occurrence of a strong cyclonic wind curl cell, associated with favourable upwelling conditions at the Hawaiian Islands. The favourable conditions for the development of a phytoplankton community dominated by large phytoplankton cells in cyclonic eddies may enhance the efficiency of the biological pump and a larger potential of carbon sequestration associated with these structures.

BGD
9, 10241–10283, 2012

4.2 Anticyclonic eddies

In contrast to cyclonic eddies we observed lower nutrient availability in anticylonic eddies related with the deepening of the nutricline and with a downward diapycnal flow. Indeed, our results documented the occurrence of anticylonic wind curl/shear regions partly responsible of the eddies generation (Jiménez et. al., 2008; Piedeleu et al., 2009) in the Canary Eddies Corridor, favouring downward Ekman pumping velocities (Jiménez et al., 2008) and downward fluxes (downwelling) as previously described (Basterretxea et al., 2002). The reduction in nutrient availability may favour the predominance of picoplanktonic forms better adapted to oligotrophic conditions (Platt et al., 1983; Agawin et al., 2000; Lasternas et al., 2010), as reflected in the dominance of *Prochlorococcus* sp. The AE stations also presented higher bacterial abundance, as reported in parallel studies conducted at the same region (Baltar et al., 2010; Boras et al., 2010).

Originally located at the vicinity of the productive Gran Canaria's current, anticyclonic eddies sampled in this study were at their early stage (attached or close to the islands, spin up stage) associated to particularly active downward processes. The strong downwelling dynamic at the AE progressively depletes the system of nutrients, influencing biological processes at the upper layers. Despite similar oligotrophic levels in FF and AE, there was no evidence of downwelling at the FF station, as wind curl was near zero and a significantly less deep mixed layer (FF1 = 25 m, FF2 = 30 m) may be as well an indicative of a less active mixing than for the AEs. The setting-up of anticyclonic eddies altered the system as indicated by higher mortality of the nano-microphytoplankton population at surface layers despite comparable abundances to CE stations. Indeed, albeit we reported here higher nano-microphytoplankton biomass at AE than FF, the percentage of dead cells was higher at the anticyclonic eddies indicative of senescence of the populations induced by the downwelling processes in the AE studied. The high variability of the nano-microphytoplankton mortality values in the water column observed at AE illustrates the system alteration, affecting the phytoplankton communities

BGD
9, 10241–10283, 2012

that are in transient from a dominance of nano-microphytoplankton to that of picophytoplankton community as indicated by the high fraction of dead diatom cells in the community. Diatoms have high nutrient requirements and are strongly impacted by nutrients depletion, particularly that of silicate (Martin-Jézéquel et al., 2000) a nutrient that clearly decreased in the AEs compared to CEs and FF stations. Dinoflagellates, which typically trhive in stratified waters condition (Smayda and Reynolds, 2001), presented high mortality at the AE (> 70 % of dead cells) further suggesting that the strongly oligotrophic conditions together downwelling and active mixing conditions in this zone offer conditions unsuitable for microphytoplankton. The picophytoplankton component showed lower cell mortality than nanomicroplankton but was also affected as the proportion of dead cells was higher in AE stations than at far field stations, which represent a likely "stable" environment for picophytoplankton groups where ecological niches are well defined (Agustí, 2004). The stressing conditions for autotrophs was reflected in high lysis rates in AE stations. Previous studies presented similar lysis rates in the area (Agustí et al., 2001), likely associated to oligotrophic conditions, but the eddy systems generated variation in those rates as well. In our study, the hydrological conditions associated with the AE, resulted in higher lysis rates than those observed in the FF and in CE, also resulting in higher P_{DOC} in AE stations. Indeed, we observed a strong relationship between phytoplankton lysis rates and P_{DOC}, emphasizing the important consequences of phytoplankton cell mortality and lysis in contributing to the extracellular dissolved organic carbon production by phytoplankton.

A high release of dissolved organic carbon produced (P_{DOC}) by the senescent phytoplankton population found in anticyclonic eddies explains the higher abundance of heterotrophic bacteria in AEs, consistent with the role of DOC as a substrate for heterotrophic bacteria growth (Kirchman et al., 1991; Norrman et al., 1995; Carlson and Ducklow, 1996; Kirchman and Rich, 1997). Despite that, Baltar et al. (2010) studied the bacterial dynamics in the same eddies system but including deeper layers down to 1000 m depth and found prokaryotic activity being significantly lower at the AE. We also found unexpected lower HB cell viability at AE despite higher P_{DOC} suggesting

BGD
9, 10241–10283, 2012

that bacteria are also affected by environmental changes at AE. Limitation by inorganic nutrients as phosphorus could influence the viability of HB (Lasternas et al., 2010). Indeed, nutrient supply has been shown to explain variability in bacterial activity in the Atlantic Ocean (Gasol et al., 2009), and the negative relationship between the %DC of *Synechococcus* sp. and the %LC of HB found here could indicate a competition for phosphorus in the eddies system (Zubkov et al., 2007; Lasternas et al., 2010). We found a significant positive relationship between bacterial cell viability and the ammonium concentration indicating that ammonium, which stimulates bacterial activity and growth efficiency (Bratbak, 1987; Kroer et al., 1993), could be another important nutrient controlling bacteria in the eddies system. Moreover, the significantly higher ammonium concentration found at AEs indicated intense recycling processes resulting in a larger regenerated production than at FF or CEs, which is in accordance with the highest pressure on bacteria by protists observed in the AEs by Boras et al. (2010).

4.3 Contrasted carbon fluxes within the eddies system and anticyclonic forcing

The results presented provide evidence that the anticyclonic system studied generated environmental perturbations stressing phytoplankton communities in the early stages of anticyclone eddy development in the Canary current region. While phytoplankton production and biomass were higher in both cyclonic and anticyclonic eddies than at waters outside the eddies (FF), biological processes were highly modified by downstream dynamics in AEs affecting biogeochemical fluxes and the pathway of photosynthetic carbon flow, largely as dissolved organic carbon, in AE.

The anticyclonic eddies studied here could be defined as transient systems between moderately productive waters and oligotrophic waters that prevail at the FF stations at this zone of the NE Atlantic. Indeed, during its formation, anticyclonic eddies are fed by productive waters generated at the Canary current, which can support higher production and biomass than the common NE Atlantic oligotrophic waters (Barton et al., 1998; Sangrà et al., 2007). However, downwelling at AEs progressively deprive the system of nutrients, resulting in a progressive oligotrophication of the eddies that favoured, in our

BGD
9, 10241–10283, 2012

study, the predominance of smaller phytoplanktonic cells and senescent populations of large photosynthetic cells.

Here, we showed that the perturbations that occurred at the early-stage anticyclonic eddies shed by the Canary Islands, mainly active downwelling, result in increased phytoplankton cell mortality, particularly affecting diatoms and other larger phytoplankton cells, influencing carbon flux (Kirchman et al., 1991; Agustí et al., 1998). Diatoms are considered to dominate the downward export flux of particulate carbon contributing significantly to the long-term sequestration of atmospheric CO_2 in the ocean interior (Smetacek, 1985, 1999; Martin et al., 2011) so the reduction of the large, rapidly sinking phytoplankton, such as diatoms population along with the increasing picophytoplankton, should weaken the biological pump capacity of AEs (Michaels and Silver, 1988; Legendre and Le Fèvre, 1995). Indeed, the increased phytoplantkton cell mortality and lysis observed here resulted in a large P_{DOC} release to the medium in the AEs, that should strongly reduce the potential for the export of carbon to the deep ocean mediated by the biological pump, favouring the microbial loop (Pomeroy, 1974; Azam et al., 1983; Legendre and Le Fèvre, 1995).

Although the consequences of the CE for the carbon fluxes have been well documented, those of anticyclonic systems remain more erratic. While the reduction of phytoplankton production and biomass in AE systems has been reported in the past (Falkowski et al., 1991; McGillicuddy et al., 1998), some AE systems have been recently described to be able to enhance phytoplankton biomass under certain conditions (McGillicuddy et al., 2007; Sangrà et al., 2009). Here, we report no different in phytoplankton production and Chl *a* concentration between AE and CE systems in the Canary eddy field. However, the oligotrophication process in AE resulting in lower nutrient concentrations in anticyclonic eddies was linked to a shift towards picoautotrophs, the senescent of microphytoplankton cells, with an overall increase in lysis rates and a relative increase in the flow of carbon to dissolved organic carbon compared to cyclonic eddies. These results highlight the importance of examining the consequences of eddy dynamics on phytoplankton cell status, which can affect phytoplankton communities

BGD
9, 10241–10283, 2012

and the partitioning of carbon flow between particulate and dissolved pathways, with fundamental consequences for carbon flow in the ocean.

Acknowledgements. This research is a contribution to the project RODA (CTM-2004-06842-CO3-O2 and O3) and the project MEDEICG (CTM2009-07013) funded by the Spanish Ministry of Science and Innovation. We thank the crew of the RV *Hespérides*' for help during the RODA cruise. S. L. was supported by a EUR-OCEANS fellowship.

References

Agawin, N. S. R., Duarte, C. M. and Agustí, S.: Nutrient and Temperature Control of the Contribution of Picoplankton to Phytoplankton Biomass and Production, Limnol. Oceanogr., 45, 591–600, 2000.

Agustí, S.: Viability and niche segregation of Prochlorococcus and Synechococcus cells across the Central Atlantic Ocean, Aquat. Microb. Ecol., 36, 53–59, doi:10.3354/ame036053, 2004.

Agustí, S. and Duarte, C. M.: Strong Seasonality in Phytoplankton Cell Lysis in the NW Mediterranean Littoral, Limnol. Oceanogr., 45, 940–947, 2000.

Agustí, S. and Sánchez, M. C.: Cell Viability in Natural Phytoplankton Communities Quantified by a Membrane Permeability Probe, Limnol. Oceanogr., 47, 818–828, 2002.

Agustí, S., Satta, M. P., Mura, M. P., and Benavent, E.: Dissolved Esterase Activity as a Tracer of Phytoplankton Lysis: Evidence of High Phytoplankton Lysis Rates in the Northwestern Mediterranean, Limnol. Oceanogr., 43, 1836–1849, 1998.

Agustí, S., Duarte, C. M., Vaqué, D., Hein, M., Gasol, J. M., and Vidal, M.: Food-web structure and elemental (C, N and P) fluxes in the eastern tropical North Atlantic, Deep-Sea Res. Pt. II, 48, 2295–2321, doi:10.1016/S0967-0645(00)00179-X, 2001.

Alonso-González, I. J., Arístegui, J., Lee, C., and Calafat, A.: Regional and temporal variability of sinking organic matter in the subtropical northeast Atlantic Ocean: a biomarker diagnosis, Biogeosciences, 7, 2101–2115, doi:10.5194/bg-7-2101-2010, 2010.

Alonso-Laita, P. and Agustí, S.: Contrasting patterns of phytoplankton viability in the subtropical NE Atlantic, Ocean. Aquat. Microb. Ecol., 43, 67–78, doi:10.3354/ame043067, 2006.

Arístegui, J. and Montero, M. F.: Temporal and spatial changes in plankton respiration and biomass in the Canary Islands region: the effect of mesoscale variability, J. Marine Syst., 54, 65–82, doi:10.1016/j.jmarsys.2004.07.004, 2005.

BGD

9, 10241–10283, 2012

Arístegui, J., Tett, P., Hernández-Guerra, A., Basterretxea, G., Montero, M. F., Wild, K., Sangrá, P., Hernández-Leon, S., Canton, M., García-Braun, J. A., Pacheco, M., and Barton, E. D.: The influence of island-generated eddies on chlorophyll distribution: a study of mesoscale variation around Gran Canaria, Deep-Sea Res. Pt. I, 44, 71–96, doi:10.1016/S0967-0637(96)00093-3, 1997.

Arístegui, J., Barton, E., Montero, M., García-Muñoz, M., and Escánez, J.: Organic carbon distribution and water column respiration in the NW Africa-Canaries Coastal Transition Zone, Aquat. Microb. Ecol., 33, 289–301, doi:10.3354/ame033289, 2003.

Baltar, F., Aristegui, J., Gasol, J. M., Lekunberri, I., and Herndl, G. J.: Mesoscale eddies: hotspots of prokaryotic activity and differential community structure in the ocean, ISME J., 4, 975–988, 2010.

Barbesti, S., Citterio, S., Labra, M., Baroni, M. D., Neri, M. G., and Sgorbati, S.: Two and three-color fluorescence flow cytometric analysis of immunoidentified viable bacteria, Cytometry, 40, 214–218, 2000.

Barton, E. D., Arìstegui, J., Tett, P., Cantón, M., Garcìa-Braun, J., Hernández-León, S., Nykjaer, L., Almeida, C., Almunia, J., Ballesteros, S., Basterretxea, G., Escánez, J., Garcìa-Weill, L., Hernández-Guerra, A., López-Laatzen, F., Molina, R., Montero, M. F., Navarro-Pérez, E., Rodrìguez, J. M., van Lenning, K., Vélez, H., and Wild, K.: The transition zone of the Canary Current upwelling region, Prog. Oceanogr., 41, 455–504, doi:10.1016/S0079-6611(98)00023-8, 1998.

Basterretxea, G., Barton, E. D., Tett, P., Sangrá, P., Navarro-Perez, E., and Arístegui, J.: Eddy and deep chlorophyl maximum response to wind-shear in the lee of Gran Canaria, Deep-Sea Res. Pt. I, 49, 1087–1101, doi:10.1016/S0967-0637(02)00009-2, 2002.

Benitez-Nelson, C. R. and McGillicuddy Jr., D. J.: Mesoscale physical–biological–biogeochemical linkages in the open ocean: An introduction to the results of the E-Flux and EDDIES programs, Deep-Sea Res. Pt. II, 55, 1133–1138, doi:10.1016/j.dsr2.2008.03.001, 2008.

Berges, J. A. and Falkowski, P. G.: Physiological Stress and Cell Death in Marine Phytoplankton: Induction of Proteases in Response to Nitrogen or Light Limitation, Limnol. Oceanogr., 43, 129–135, 1998.

Bidigare, R. R., Benitez-Nelson, C., Leonard, C. L., Quay, P. D., Parsons, M. L., Foley, D. G., and Seki, M. P.: Influence of a cyclonic eddy on microheterotroph biomass and carbon export in the lee of Hawaii, Geophys. Res. Lett., 30, 1318, doi:10.1029/2002GL016393, 2003.

BGD
9, 10241–10283, 2012

Boras, J. A., Sala, M. M., Baltar, F., Aristegui, J., Duarte, C. M., and Vaqué, D.: Effect of viruses and protists on bacteria in eddies of the Canary Current region (subtropical northeast Atlantic), Limnol. Oceanogr., 55, 885–898, 2010.
Bratbak, G.: Carbon flow in an experimental microbial ecosystem, Mar. Ecol. Prog. Ser., 36, 267–276, 1987.
Brussaard, C. P. D., Riegman, R., Noordeloos, A. A. M., Cadée, G. C., Witte, H., Kop, A. J., Nieuwland, G., Van Duyl, F. C., and Bak, R. P. M.: Effects of grazing, sedimentation and phytoplankton cell lysis on the structure of a coastal pelagic food web, Mar. Ecol. Prog. Ser., 123, 259–271, 1995.
Carlson, C. and Ducklow, H.: Growth of bacterioplankton and consumption of dissolved organic carbon in the Sargasso Sea, Aquat. Microb. Ecol., 10, 69–85, doi:10.3354/ame010069, 1996.
Ewart, C. S., Meyers, M. K., Wallner, E. R., McGillicuddy Jr., D. J., and Carlson, C. A.: Microbial dynamics in cyclonic and anticyclonic mode-water eddies in the northwestern Sargasso Sea, Deep-Sea Res. Pt. II, 55, 1334–1347, doi:10.1016/j.dsr2.2008.02.013, 2008.
Falcioni, T., Papa, S., and Gasol, J. M.: Evaluating the Flow-Cytometric Nucleic Acid Double-Staining Protocol in Realistic Situations of Planktonic Bacterial Death, Appl. Environ. Microbiol., 74, 1767–1779, doi:10.1128/AEM.01668-07, 2008.
Falkowski, P. G., Ziemann, D., Kolber, Z., and Bienfang, P. K.: Role of eddy pumping in enhancing primary production in the ocean, Nature, 352, 55–58, doi:10.1038/352055a0, 1991.
Garçon, V. C., Oschlies, A., Doney, S. C., McGillicuddy Jr., D. J., and Waniek, J.: The role of mesoscale variability on plankton dynamics in the North Atlantic, Deep-Sea Res. Pt. II, 48, 2199–2226, doi:10.1016/S0967-0645(00)00183-1, 2001.
Gasol, J. M., Vázquez-Domínguez, E., Vaqué, D., Agustí, S., and Duarte, C. M.: Bacterial activity and diffusive nutrient supply in the oligotrophic Central Atlantic Ocean, Aquat. Microb. Ecol., 56, 1–12, doi:10.3354/ame01310, 2009.
González-Dávila, M., Santana-Casiano, J. M., de Armas, D., Escánez, J., and Suarez-Tangil, M.: The influence of island generated eddies on the carbon dioxide system, south of the Canary Islands, Mar. Chem., 99, 177–190, doi:10.1016/j.marchem.2005.11.004, 2006.
Grégori, G., Citterio, S., Ghiani, A., Labra, M., Sgorbati, S., Brown, S., and Denis, M.: Resolution of Viable and Membrane-Compromised Bacteria in Freshwater and Marine Waters Based on Analytical Flow Cytometry and Nucleic Acid Double Staining, Appl. Environ. Microbiol., 67, 4662–4670, doi:10.1128/AEM.67.10.4662-4670.2001, 2001.

BGD
9, 10241–10283, 2012

Hansen, H. P. and Koroleff, F.: Determination of nutrients, in: Methods of seawater analysis, edited by: Grasshoff, K., Kremling, K., and Ehrhardt, M., Weinheim, Wiley-VCH Verlag, 159–228, 1999.
Hart, J. E.: On nonlinear Ekman surface-layer pumping, J. Phys. Oceanogr., 26, 1370–1374, 1996.
Jia, Y., Calil, P. H. R., Chassignet, E. P., Metzger, E. J., Potemra, J. T., Richards, K. J., and Wallcraft, A. J.: Generation of mesoscale eddies in the lee of the Hawaiian Islands, J. Geophys. Res., 116, C11009, doi:201110.1029/2011JC007305, 2011.
Jiménez, B., Sangrà, P., and Mason, E.: A numerical study of the relative importance of wind and topographic forcing on oceanic eddy shedding by tall, deep water islands, Ocean Model., 22, 146–157, 2008.
Kara, A. B., Rochford, P. A., and Hurlburt, H. E.: An optimal definition for ocean mixed layer depth, J. Geophys. Res., 105, 16803–16821, doi:200010.1029/2000JC900072, 2000.
Kérouel, R. and Aminot, A.: Fluorometric determination of ammonia in sea and estuarine waters by direct segmented flow analysis, Mar. Chem., 57, 265–275, 1997.
Kirchman, D. L. and Rich, J. H.: Regulation of Bacterial Growth Rates by Dissolved Organic Carbon and Temperature in the Equatorial Pacific Ocean, Microb. Ecol., 33, 11–20, doi:10.1007/s002489900003, 1997.
Kirchman, D. L., Suzuki, Y., Garside, C., and Ducklow, H. W.: High turnover rates of dissolved organic carbon during a spring phytoplankton bloom, Nature, 352, 612–614, doi:10.1038/352612a0, 1991.
Kroer, N.: Bacterial Growth Efficiency on Natural Dissolved Organic Matter, Limnol. Oceanogr., 38, 1282–1290, 1993.
Lasternas, S., Agustí, S., and Duarte, C. M.: Phyto- and bacterioplankton abundance and viability and their relationship with phosphorus across the Mediterranean Sea, Aquat. Microb. Ecol., 60, 175–191, doi:10.3354/ame01421, 2010.
Legendre, L. and Le Fèvre, J.: Microbial food webs and the export of biogenic carbon in oceans, Aquat. Microb. Ecol., 9, 69–77, 1995.
Llabrés, M. and Agustí, S.: Picophytoplankton Cell Death Induced by UV Radiation: Evidence for Oceanic Atlantic Communities, Limnol. Oceanogr., 51, 21–29, 2006.
Mahadevan, A., Thomas, L. N., and Tandon, A.: Comment on "Eddy/Wind Interactions Stimulate Extraordinary Mid-Ocean Plankton Blooms", Science, 320, 448–448, doi:10.1126/science.1152111, 2008.

BGD
9, 10241–10283, 2012

Marie, D., Simon, N., and Vaulot, D.: Phytoplankton cell counting by flow cytometry, Algal Culturing Techniques, 253–268, 2005.
Martin, A. P. and Richards, K. J.: Mechanisms for vertical nutrient transport within a North Atlantic mesoscale eddy, Deep-Sea Res. Pt. II, 48, 757–773, doi:10.1016/S0967-0645(00)00096-5, 2001.
Martin, P., Lampitt, R. S., Jane Perry, M., Sanders, R., Lee, C., and D'Asaro, E.: Export and mesopelagic particle flux during a North Atlantic spring diatom bloom, Deep-Sea Res. Pt. I, 58, 338–349, doi:10.1016/j.dsr.2011.01.006, 2011.
Martin-Jézéquel, V., Hildebrand, M., and Brzezinski, M. A.: Silicon metabolism in diatoms: Implications for growth, J. Phycol., 36, 821–840, doi:10.1046/j.1529-8817.2000.00019.x, 2003.
Mason, E., Colas, F., Molemaker, J., Shchepetkin, A. F., Troupin, C., McWilliams, J. C., and Sangrà, P.: Seasonal variability of the Canary Current: A numerical study, J. Geophys. Res., 116, C06001, doi:201110.1029/2010JC006665, 2011.
Mathis, J. T., Pickart, R. S., Hansell, D. A., Kadko, D., and Bates, N. R.: Eddy transport of organic carbon and nutrients from the Chukchi Shelf: Impact on the upper halocline of the western Arctic Ocean, J. Geophys. Res., 112, C05011, doi:10.1029/2006JC003899, 2007.
McGillicuddy Jr., D. J., Robinson, A. R., Siegel, D. A., Jannasch, H. W., Johnson, R., Dickey, T. D., McNeil, J., Michaels, A. F., and Knap, A. H.: Influence of mesoscale eddies on new production in the Sargasso Sea, Nature, 394, 263–266, 1998.
McGillicuddy Jr., D. J., Johnson, M., R., Siegel, D. A., Michaels, A. F., Bates, N. R., and Knap, A. H.: Mesoscale variations of biogeochemical properties in the Sargasso Sea, J. Geophys. Res., 104, 13381–13394, doi:199910.1029/1999JC900021, 1999.
McGillicuddy Jr., D. J., Anderson, L. A., Bates, N. R., Bibby, T., Buesseler, K. O., Carlson, C. A., Davis, C. S., Ewart, C., Falkowski, P. G., Goldthwait, S. A., Hansell, D. A., Jenkins, W. J., Johnson, R., Kosnyrev, V. K., Ledwell, J. R., Li, Q. P., Siegel, D. A., and Steinberg, D. K.: Eddy/Wind Interactions Stimulate Extraordinary Mid-Ocean Plankton Blooms, Science, 316, 1021–1026, doi:10.1126/science.1136256, 2007.
McGillicuddy Jr., D. J., Ledwell, J. R., and Anderson, L. A.: Response to Comment on "Eddy/Wind Interactions Stimulate Extraordinary Mid-Ocean Plankton Blooms", Science, 320, p. 448, doi:10.1126/science.1148974, 2008.
McNeil, J. D., Dickey, T., Jannasch, H. W., Sakamoto, C. M., McGillicuddy Jr., D. J., and Brzezinski, M.: New chemical, bio-optical and physical observations of upper ocean response to the passage of a mesoscale eddy off Bermuda, J. Geophys. Res., 104, 15537–15548, 1999.

BGD
9, 10241–10283, 2012

Michaels, A. F. and Silver, M. W.: Primary production, sinking fluxes and the microbial food web, Deep-Sea Res., 35, 473–490, doi:10.1016/0198-0149(88)90126-4, 1988.
Myklestad, S.: Production of carbohydrates by marine planktonic diatoms. II. Influence of the ratio in the growth medium on the assimilation ratio, growth rate, and production of cellular and extracellular carbohydrates by Chaetoceros affinis var. willei (Gran) Hustedt and Skeletonema costatum (Grev.) Cleve, J. Exp. Mar. Biol. Ecol., 29, 161–179, doi:10.1016/0022-0981(77)90046-6, 1977.
Norrman, B., Zweifel, U. L., Hopkinson, C. S., and Fry, B.: Production and utilization of dissolved organic carbon during an experimental diatom bloom, Limnol. Oceanogr., 40, 898–907, 1995.
Oschlies, A. and Garçon, V.: Eddy-induced enhancement of primary production in a model of the North Atlantic Ocean, Nature, 394, 266–269, 1998.
Owen, R. W.: Fronts and eddies in the sea: mechanisms, interactions and biological effects, in: Analysis of marine ecosystems, edited by: Longhurst, A. R., Academic Press, New York, 197–233, 1981.
Pallàs-Sanz, E., Johnston, T. M. S., and Rudnick, D. L.: Frontal dynamics in a California Current System shallow front: 1. Frontal processes and tracer structure, J. Geophys. Res., 115, C12067, doi:10.1029/2009JC006032, 2010.
Parsons, T. R., Maita, Y., and Lalli, C. M.: A manual of chemical and biological methods for seawater analysis, Pergamon Press, Oxford, 1984.
Piedeleu, M., Sangrà, P., Sánchez-Vidal, A., Fabrés, J., Gordo, C., and Calafat, A.: An observational study of oceanic eddy generation mechanisms by tall deep-water islands (Gran Canaria), Geophys. Res. Lett., 36, L14605, doi:200910.1029/2008GL037010, 2009.
Platt, T., Rao, D. V. S., and Irwin, B.: Photosynthesis of picoplankton in the oligotrophic ocean, Nature, 301, 702–704, doi:10.1038/301702a0, 1983.
Pomeroy, L. R.: The ocean's foodweb: a changing paradigm, Bioscience, 24, 499–504, 1974.
Proctor, L. M. and Fuhram, J. A.: Roles of viral infection in organic particle flux, Marine, 69, 133–142, 1991.
Rodríguez, F., Varela, M., Fernández, E., and Zapata, M.: Phytoplankton and pigment distributions in an anticyclonic slope water oceanic eddy (SWODDY) in the southern Bay of Biscay, Mar. Biol., 143, 995–1011, doi:10.1007/s00227-003-1129-1, 2003.

BGD
9, 10241–10283, 2012

Rodríguez, J., Tintore, J., Allen, J. T., Blanco, J. M., Gomis, D., Reul, A., Ruiz, J., Rodríguez, V., Echevarria, F., and Jiménez-Gomez, F.: Mesoscale vertical motion and the size structure of phytoplankton in the ocean, Nature, 410, 360–363, doi:10.1038/35066560, 2001.

Sangrà, P., Pelegri, J. L., Hernández-Guerra, A., Arregui, I., Martín, J. M., Marrero-Díaz, A., Martínez, A., Ratsimandresey, A. W., and Rodríguez-Santana, A.: Life history of an anticyclonic eddy, J. Geophys. Res., 110, C03021, doi:10.1029/2004JC002526, 2005.

Sangrà, P., Auladell, M., Marrero-Díaz, A., Pelegrí, J. L., Fraile-Nuez, E., Rodríguez-Santana, A., Martín, J. M., Mason, E., and Hernández-Guerra, A.: On the nature of oceanic eddies shed by the Island of Gran Canaria, Deep-Sea Res. Pt. I, 54, 687–709, doi:10.1016/j.dsr.2007.02.004, 2007.

Sangrà, P., Pascual, A., Rodríguez-Santana, A., Machín, F., Mason, E., McWilliams, J. C., Pelegrí, J. L., Dong, C., Rubio, A., Arístegui, J., Marrero-Díaz, Á., Hernández-Guerra, A., Martínez-Marrero, A., and Auladell, M.: The Canary Eddy Corridor: A major pathway for long-lived eddies in the subtropical North Atlantic, Deep-Sea Res. Pt. I, 56, 2100–2114, doi:10.1016/j.dsr.2009.08.008, 2009.

Siegel, S. and Castellan, N. J.: Non-parametric statistics for the behavioural sciences, McGraw Hill Company, New York, 1988.

Siegel, D. A, McGillicuddy, D. J., and Fields, E. A.: Mesoscale eddies, satellite altimetry, and new production in the Sargasso Sea, J. Geophys. Res., 104, 13359–13379, 1999.

Smayda, T. J. and Reynolds, C. S.: Community assembly in marine phytoplankton: Application of recent models to harmful dinoflagellate blooms, J. Plankton Res., 23, 447–461, doi:10.1093/plankt/23.5.447, 2001.

Smetacek, V. S.: Role of sinking in diatom life-history cycles: ecological, evolutionary and geological significance, Mar. Biol., 84, 239–251, doi:10.1007/BF00392493, 1985.

Smetacek, V. S.: Diatoms and the ocean carbon cycle, Protist, 250, 25–32, 1999.

Smith, C. L., Richards, K. J., and Fasham, M. J. R.: The impact of mesoscale eddies on plankton dynamics in the upper ocean, Deep-Sea Res. Pt. I, 43, 1807–1832, doi:10.1016/S0967-0637(96)00035-0, 1996.

Steemann-Nielsen, E. J.: The use of radioactive carbon (l4C) for measuring organic production in the sea, Cons. Perm. Int. Explor. Mer., 18, 117–140, 1952.

Tarran, G. A., Zubkov, M. V., Sleigh, M. A., Burkill, P. H., and Yallop, M.: Microbial community structure and standing stocks in the NE Atlantic in June and July of 1996, Deep-Sea Res. Pt. II, 48, 963–985, doi:10.1016/S0967-0645(00)00104-1, 2001.

BGD
9, 10241–10283, 2012

Vaillancourt, R. D., Marra, J., Seki, M. P., Parsons, M. L., and Bidigare, R. R.: Impact of a cyclonic eddy on phytoplankton community structure and photosynthetic competency in the subtropical North Pacific Ocean, Deep-Sea Res. Pt. I, 50, 829–847, doi:10.1016/S0967-0637(03)00059-1, 2003.

Zubkov, M. V., Mary, I., Woodward, E. M. S., Warwick, P. E., Fuchs, B. M., Scanlan, D. J., and Burkill, P. H.: Microbial control of phosphate in the nutrient-depleted North Atlantic subtropical gyre, Environ. Microbiol., 9, 2079–2089, doi:10.1111/j.1462-2920.2007.01324.x, 2007.

BGD
9, 10241–10283, 2012

Table 1. Oceanographic properties characterizing the structure of cyclonic and anticyclonic eddies (CE and AEs, respectively), studied. T-anomaly and H-anomaly correspond to the temperature anomaly and dynamic height anomalies, respectively.

EDDY	CE1	CE2	AE1	AE2
Origin	Gran Canaria	La Palma	El hierro	Gran Canaria
Eddy Type	Cyclonic	Cyclonic	Anticyclonic	Anticyclonic
Data type	CTD	XBT-CTD(L)	XBT	XBT
T-anomaly	−4 °C (50 m)	−4.56 °C (50 m)	3.5 °C (140 m)	4,5 °C (70 m)
H-anomaly	−77 m	−64 m	73 m	65 m
Depth	> 500 m	350 m	350 m	300 m
Mixing layer depth	20 m	30 m	160 m	90 m

BGD
9, 10241–10283, 2012

Table 2. Average ± SE (range) nutrient concentration, temperature and chlorophyll *a* in the cyclonic and anticyclonic eddies (CE and AEs, respectively) and far field stations studied. Average values for systems connected by different letters are significantly different ($p < 0.05$).

Variable	Anticyclonic eddies	Cyclonic eddies	Far fields
DIP (µM)	0.05 ± 0.03^{b} (0.001–0.25)	0.29 ± 0.03^{a} (0.08–0.36)	0.001 ± 0.00^{b} (0.001–0.001)
Silicate (µM)	0.44 ± 0.04^{b} (0.23–0.58)	0.69 ± 0.12^{a} (0.21–1.27)	0.69 ± 0.03^{a} (0.55–0.83)
DIN (µM)	0.26 ± 0.12^{b} (0.04–0.85)	1.21 ± 0.47^{a} (0.08–3.97)	0.14 ± 0.05^{b} (0.06–0.49)
Ammonium (µM)	1.26 ± 0.21^{a} (0.36–2.18)	0.28 ± 0.04^{b} (0.18–0.41)	0.72 ± 0.15^{b} (0.09–1.33)
Temperature (°C)	22.4 ± 0.5^{a} (19.6–24.0)	19.8 ± 0.8^{b} (17.3–23.1)	21.9 ± 0.8^{a} (18.5–24.8)
Chlorophyll *a* (mg Chl *a* mg^{-3})	0.26 ± 0.05^{b} (0.07–0.49)	0.52 ± 0.13^{a} (0.13–1.38)	0.25 ± 0.06^{b} (0.11–0.72)

BGD
9, 10241–10283, 2012

Table 3. Abundance of the microphytoplankton groups (average ± SE) in the cyclonic and anticyclonic eddies (CE and AEs, respectively) and far field stations studied. Average values for systems connected by different letters are significantly different ($p < 0.05$).

Average ± SE (cells l^{-1})	Anticyclonic eddies	Cyclonic eddies	Far fields
Nano-microphytoplankton	$3.3 \pm 0.1 \times 10^{3\,b}$	$6.4 \pm 1.2 \times 10^{3\,a}$	$1.5 \pm 0.3 \times 10^{3\,b}$
Nanoflagellates	$1.6 \pm 0.5 \times 10^{3\,ab}$	$2.3 \pm 0.6 \times 10^{3\,a}$	$6.6 \pm 0.2 \times 10^{2\,b}$
Diatoms	$6.4 \pm 1.8 \times 10^{2\,ab}$	$1.3 \pm 0.5 \times 10^{3\,a}$	$1.8 \pm 0.4 \times 10^{2\,b}$
Dinoflagellates	$2.0 \pm 0.3 \times 10^{2\,b}$	$7.6 \pm 1.1 \times 10^{2\,a}$	$2.2 \pm 0.6 \times 10^{2\,b}$

BGD
9, 10241–10283, 2012

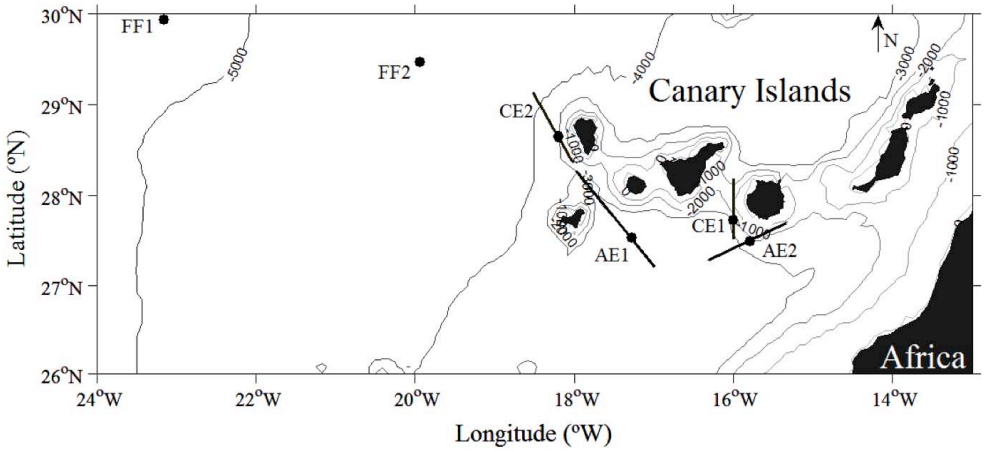

Fig. 1. Observational domain. Black dots indicate the location of the biogeochemical stations at the far field (FF1, FF2) and at the center of the cyclonic eddies (CE1, CE2) and anticyclonic eddies (AE, AE2). Black lines indicate the location of the XBTs transects crossing the eddies.

BGD
9, 10241–10283, 2012

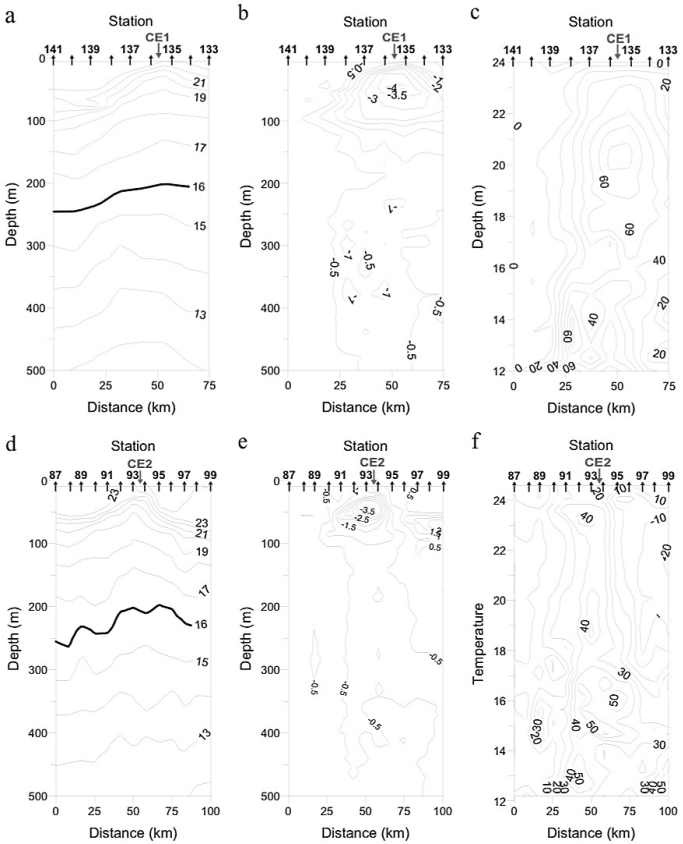

Fig. 2. Vertical sections from XBT transects showing the signals of cyclonic eddies CE1 and CE2. Left panels, temperature (˚C) section for **(a)** CE1 and **(d)** for CE2. Center panels, temperature anomaly (˚C) sections for **(b)** CE1 and **(e)** CE2. Right panels, depth anomaly sections (m) for **(c)** CE1 and **(f)** CE2. Grey arrow in the top axes indicates the location of the eddy center signal.

BGD
9, 10241–10283, 2012

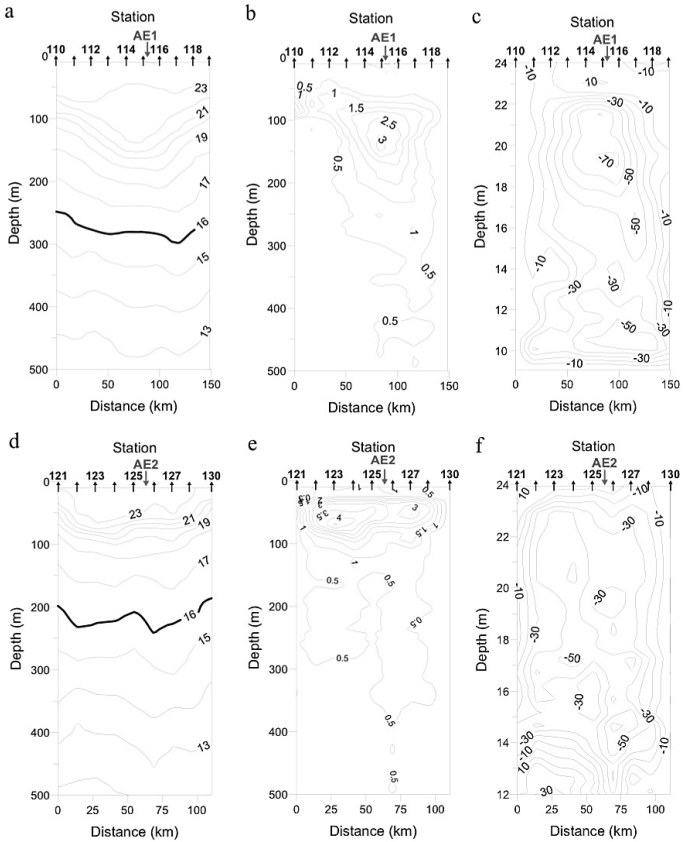

Fig. 3. Vertical sections from XBT transects showing the signals of anticyclonic eddies AE1 and AE2. Left panels, temperature (°C) section for **(a)** AE1 and **(d)** for AE2. Center panels, temperature anomaly (°C) sections for **(b)** AE1 and **(e)** AE2. Right panels, depth anomaly sections (m) for **(c)** AE1 and **(f)** AE2. Grey arrow in the top axes indicates the location of the eddy center signal.

BGD
9, 10241–10283, 2012

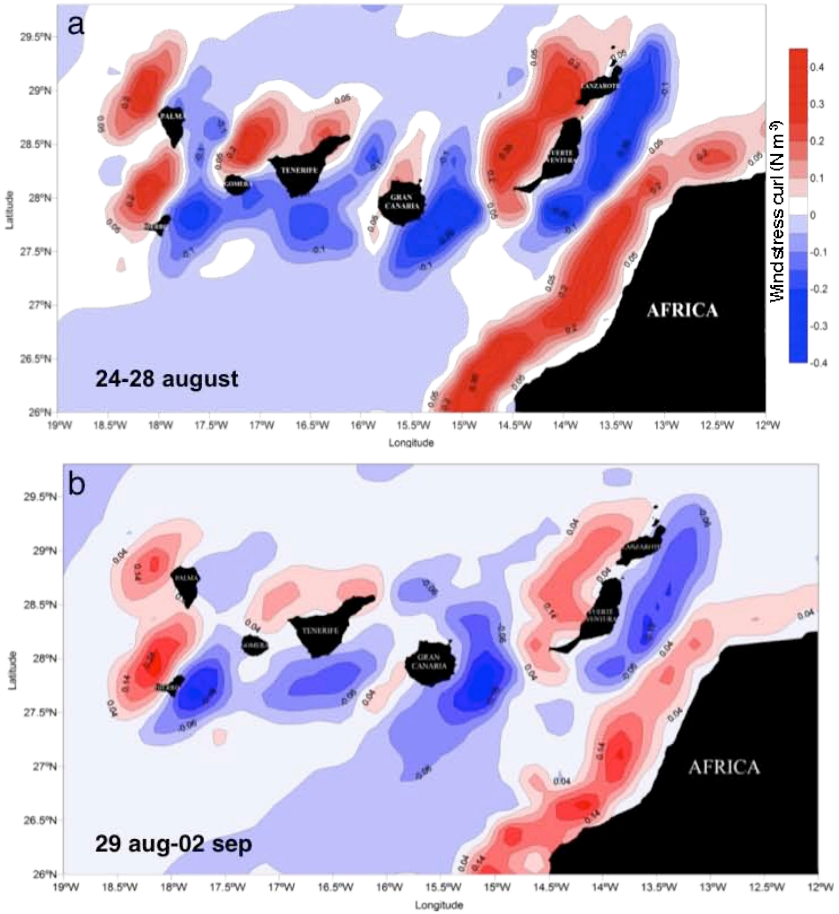

Fig. 4. Five-day averaged wind curl **(a)**, **(b)** and instantaneous wind field from the onboard meteorological station **(c)**.

BGD
9, 10241–10283, 2012

Carbon fluxes forced by anticyclonic mesoscale eddies

S. Lasternas et al.

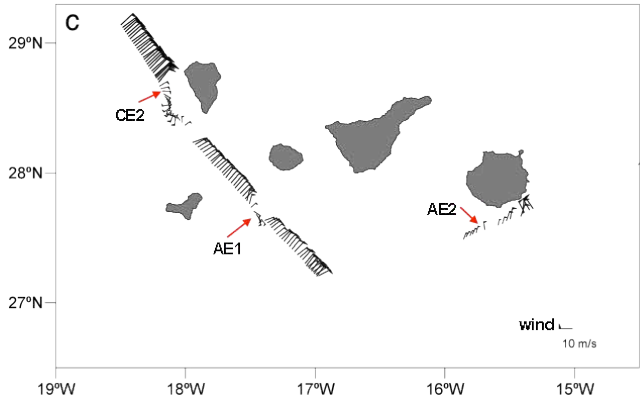

Fig. 4. Continued.

BGD
9, 10241–10283, 2012

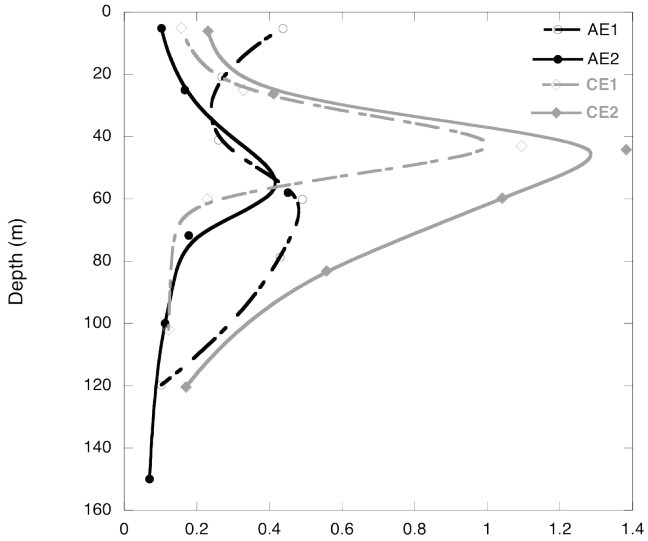

Fig. 5. Chlorophyll *a* depth profiles at the two Anticyclonic eddies (AE1–AE2) and at the two Cyclonic eddies (CE1–CE2).

BGD
9, 10241–10283, 2012

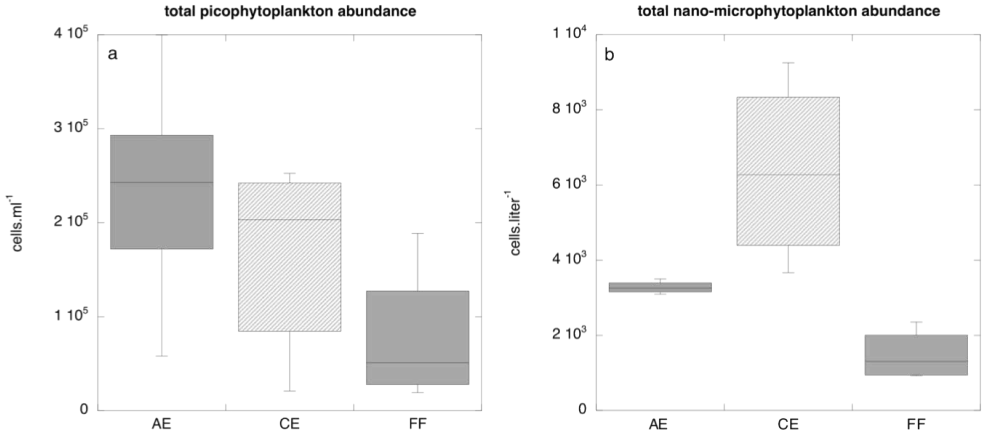

Fig. 6. Distribution of the total pico **(a)** and nano-microphytoplankton **(b)** within anticyclonic eddies (AE), cyclonic eddies (CE) and far-field stations (FF). Boxes show the lower and upper quartiles, median, minimum and maximum values.

BGD
9, 10241–10283, 2012

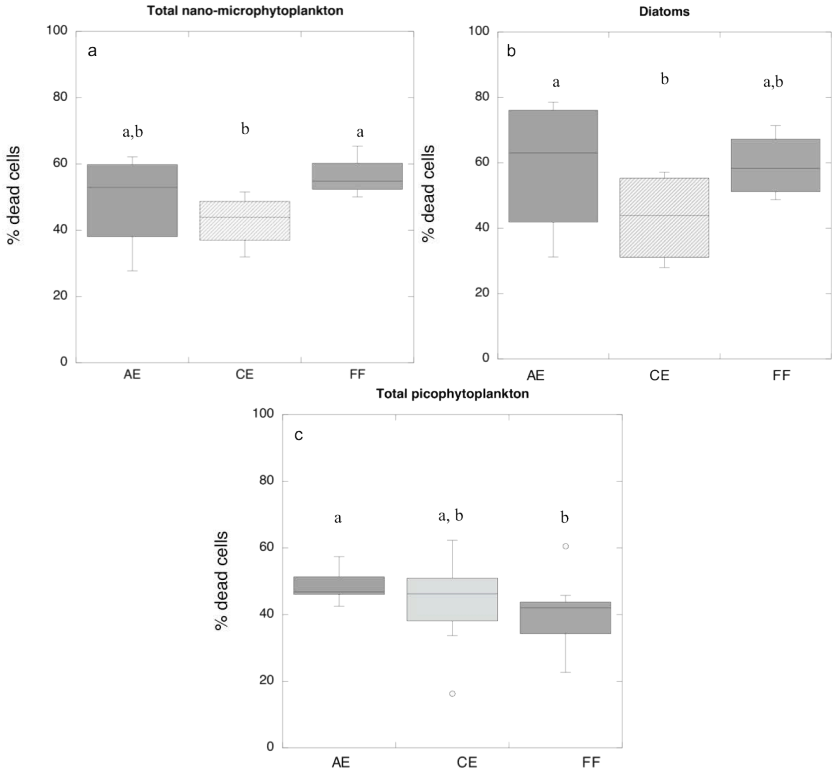

Fig. 7. Distribution of the mortality (percentage of dead cells) of **(a)** total nano-microphytoplankton, **(b)** diatoms and **(c)** total picoplankton populations within within anticyclonic eddies (AE), cyclonic eddies (CE) and far-field stations (FF). Boxes show the lower and upper quartiles, median, minimum and maximum values, and outliers (open circles). Boxes connected by same letter are not significantly different ($p < 0.05$).

BGD
9, 10241–10283, 2012

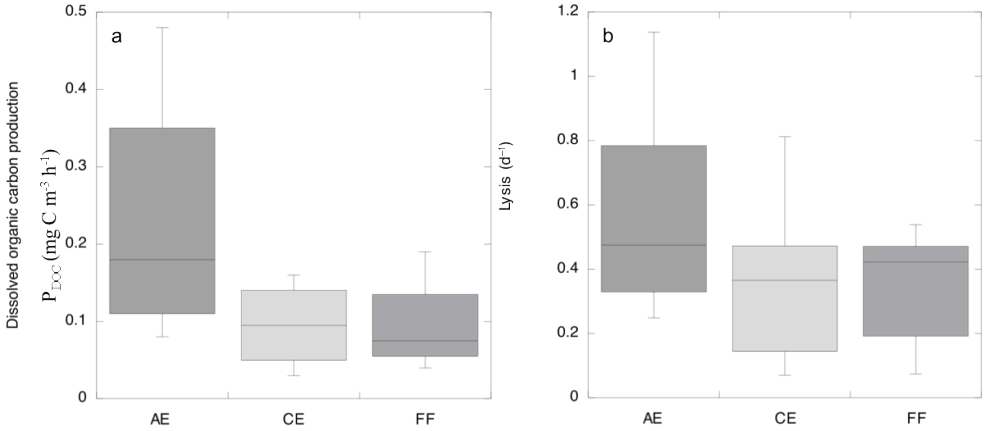

Fig. 8. Distribution of **(a)** the dissolved organic carbon production by phytoplankton (P_{DOC}), and **(b)** the lysis rates within anticyclonic eddies (AE), cyclonic eddies (CE) and far-field stations (FF). Boxes show the lower and upper quartiles, median, minimum and maximum values, and outliers (open circles).

BGD
9, 10241–10283, 2012

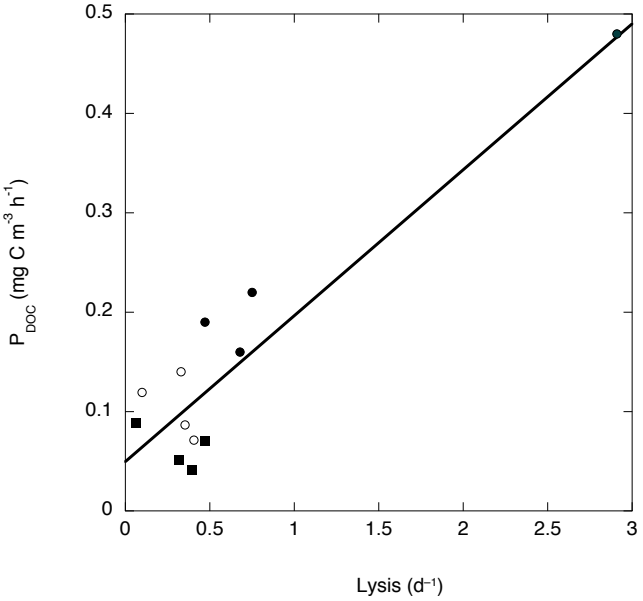

Fig. 9. The relationship found between dissolved organic carbon production by phytoplankton and lysis rates. The bold line shows the fitted regression equation $P_{DOC} = 0.05 + 0.15$ (±0.02) Lysis ($R^2 = 0.77$, $p < 0.0005$). Data from AEs (full circles), CEs (open circles) and FF (full squares).

BGD
9, 10241–10283, 2012

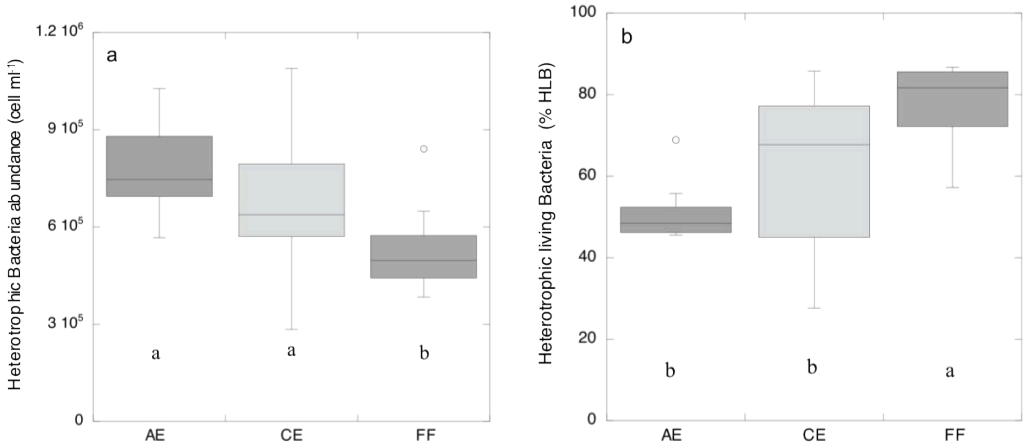

Fig. 10. Distribution of **(a)** the abundance and **(b)** viability (percentage of living cells) of the heterotrophic bacteria within anticyclonic eddies (AE), cyclonic eddies (CE) and far-field stations (FF). Boxes show the lower and upper quartiles, median, minimum and maximum values, and outliers (open circles). Boxes connected by same letter are not significantly different ($p < 0.05$).

BGD
9, 10241–10283, 2012